Accepted Manuscript

Effect of synergistic environmental conditions on thermal properties of a cold curing epoxy resin

Hamid Maljaee, Bahman Ghiassi, Paulo B. Lourenço

PII: S1359-8368(16)31676-6

DOI: 10.1016/j.compositesb.2017.01.027

Reference: JCOMB 4838

To appear in: *Composites Part B*

Received Date: 20 August 2016

Revised Date: 24 November 2016

Accepted Date: 22 January 2017

Please cite this article as: Maljaee H, Ghiassi B, Lourenço PB, Effect of synergistic environmental conditions on thermal properties of a cold curing epoxy resin, *Composites Part B* (2017), doi: 10.1016/j.compositesb.2017.01.027.

Effect of synergistic environmental conditions on thermal properties of a cold curing epoxy resin

Hamid Maljaee*, Bahman Ghiassi[1], Paulo B. Lourenço[2]

ISISE, University of Minho, Department of Civil Engineering, Guimarães, Portugal

ABSTRACT

This study presents an investigation addressing the effect of environmental conditions on the thermal properties of a cold curing epoxy resin used in repair and strengthening of masonry structures. The exposure conditions consist of laboratory indoor conditions (IC), long-term water immersion (WI), hygrothermal exposure (HG) and outdoor real exposure conditions (OC). The changes in the glass transition temperature, T_g, relaxation enthalpy and enthalpy peak temperature are monitored with Differential Scanning Calorimetry (DSC). Different measurement techniques for obtaining the T_g from DSC curves are also presented and discussed. The results showed a reduction of T_g in WI tests due to plasticization, which reversed at long-term periods. In HG conditions, post-curing of epoxy resin led to an increment of T_g. It was observed that the changes of T_g in OC conditions in the studied environment have a good correlation with the moisture absorption level and the obtained results from WI tests.

Keywords: *Epoxy resin, cold-curing, environmental degradation, thermal properties, DSC.*

* Corresponding author, PhD Student, ISISE, University of Minho, Department of Civil Engineering, Azurém, 4800-058 Guimarães, Portugal. Phone: +351 253 510 499, fax: +351 253 510 217, E-mail: h.maljaee.civil@gmail.com

[1] Marie Curie IF postdoctoral fellow, (1) Currently Department of Civil Engineering and Geosciences, TU Delft, The Netherlands; (2) ISISE, University of Minho, Department of Civil Engineering, Azurém, 4800-058 Guimarães, Portugal. E-mail: bahmanghiassi@gmail.com

[2] Professor, ISISE, University of Minho, Department of Civil Engineering, Azurém, 4800-058 Guimarães, Portugal. Phone: +351 253 510 209, fax: +351 253 510 217, E-mail: pbl@civil.uminho.pt

1 Introduction

Cold-curing thermoset epoxy resins have been extensively used in construction industry and rehabilitation projects as the matrix of structural composites or as the adhesive for externally bonded reinforcements and bonded joints. These polymers cure at low temperatures, i.e. they do not need a heat source for curing, have a relatively long curing process and have reasonable mechanical and bond properties. Epoxy resins are, however, susceptible to environmental conditions. Changes in mechanical properties and integrity, which can affect the performance of the bonded systems, have been reported as a result of exposure to environmental agents [1–8].

The most common exposure conditions in civil engineering structures are concurrent moisture and temperature variations, also called hygrothermal conditions. Many studies have focused on the effect of moisture and temperature (in an uncoupled or coupled manner) on the epoxy resins and the knowledge on curing kinetics and degradation mechanisms are rapidly growing [9–14]. The effect of moisture and hygrothermal conditions on the bond performance in FRPs bonded to concrete, to steel [15–19], and more recently to masonry [3,4,20,21] have also been under investigation.

The polymer network of epoxies is formed from the reaction of a monomer, as the responsible for polymerization, and a hardener. Once they are mixed in the liquid state, the cross linking process starts and the overall molecular structure becomes rigid (amorphous). Due to the locked-shape of the amorphous molecular structures, a significant free volume is formed in the linear network of epoxy. Epoxy resins, in chemical point of view, are cross-linked polymers. This implies that epoxies are initially in non-equilibrium state and as the crosslinking continues progressively higher equilibrium degrees are achieved. However, a full degree of curing may never be achieved when the epoxy is cured in low temperatures (i.e. natural environmental

conditions). With increasing the curing degree, the free volume and the molecular mobility in the polymer network decrease. This leads to increment of the cross-linking density and consequently the glass transition temperature, T_g [5,22].

By continuation of curing reaction in epoxy resins, the T_g surpasses the cure temperature (T_c). The time in which the T_g becomes equal to the cure temperature is called vitrification time. Vitrification is referred to a stage in which the polymer transforms from the a liquid or rubbery state to a glassy solid [23]. When epoxy resin is kept in the isothermal curing conditions with temperatures below $T_{g\infty}$ (T_g of the fully-cured epoxy resin), the epoxy resin is thermodynamically non-equilibrium and tends to evolve toward an equilibrium state. This gradual transition is known as structural relaxation process or physical ageing [5,23,24], and is accompanied with molecular rearrangements in the structure. The consequence of physical ageing process in a polymeric network is reduction of free volume, the so-called densification process, and leads to increment of relaxation times in epoxy resin [25]. Physical ageing is also associated with reversible changes in mechanical and physical properties of materials. In general, elastic modulus of epoxy resin increases with physical ageing [22,26]. The traces of physical ageing can be identified in Differential Scanning Calorimetry (DSC) test results. In the DSC curves, the endothermic ageing peak and relaxation enthalpy which usually occur near the glass transition temperature (T_g) are the evidences of the physical aging in thermoset cold-curing epoxies [25].

The changes of epoxy resins in hygrothermal conditions are the result of several complex and interrelated mechanisms. Moisture absorption can cause reversible (plasticization) and irreversible (hydrolysis, cracking and crazing) changes in physical, chemical and mechanical properties of epoxy resins. Moisture leads to increment of free volume in cross-link chain and subsequently depression of glass transition temperature (T_g) [27,28]. This process, also called

plasticization, is a physical aging mechanism and be reversed upon drying. Long-term exposure to moisture can however lead to chemical changes in the polymeric ester linkage (chemical aging) [29], and in some cases can lead to further cross-linking in the epoxy resin (thus increment of T_g). The effect of curing temperature and time on the mechanical and physical properties of thermoset resins has been extensively investigated and reported, see e.g. [30–32]. In thermosets which are not-fully cross-linked, exposure to temperatures above the curing temperature (T_c) leads to post-curing of the epoxy resins. The post-curing is usually reflected in increment of T_g up to reaching the T_g of the fully-cured epoxy resin ($T_{g\infty}$). It is worth noting that exposure to temperatures above $T_{g\infty}$ can lead to reduction of T_g and thermal degradation in thermosets [26,33]. Temperature elevations can also lead to increment of moisture absorption rate and thus faster plasticization [34].

Reduction of T_g as a result of environmental conditions can be critical especially in cold-curing epoxies that their T_g is only few degrees above the ambient temperature. The mechanical properties of epoxy resins reduce significantly at temperatures, near or above T_g which can lead to failure of structural components [35]. For this reason, several design codes have established limitations for the minimum acceptable T_g with respect to the environment's temperature. A clear understanding of the changes of T_g in different environmental conditions and development of suitable predictive models is thus be critical for service life performance prediction of composites or bonded structures.

Another challenge is the suitability of accelerated aging tests in replicating the real environmental conditions. Accelerated aging tests are generally performed at elevated temperatures or increased rate of load application that can produce unrealistic degradation mechanisms. Monitoring the changes of T_g during the accelerated aging tests and comparison

with short-term real exposure tests can be a suitable method for reliability assessment of the tests.

The aim of this paper is to investigate the effect of accelerated and real exposure conditions on the curing and thermal behavior of a typical epoxy resin used for strengthening of masonry and historical structures. Differential Scanning Calorimetry (DSC) tests are used for tracing the changes of glass transition temperature with exposure period. The accelerated exposure conditions are chosen among the most common test methods adopted by researchers but also with the aim of isolating the effect of different degrading mechanisms. The considered exposure conditions include indoor laboratory conditions (IC), water immersion at constant temperature (WI), hygrothermal conditions (HG), and outdoor real exposure conditions (OC). The effect of measurement technique for obtaining the T_g from DSC curves, another challenge for researchers and engineers, has also been deeply investigated and presented.

2 Experimental program

2.1 Materials and specimens

A commercial medium density epoxy resin (Mapei MapeWrap 31) representative of common adhesive used for preparation and application of FRPs in strengthening and rehabilitation projects, was selected in this study. This epoxy resin had two components including part A as a base resin (composed of bisphenol-A epichlorhydrin and hexanediol diglycidyl ether) and part B as a hardener (composed of m-xylylenediamine), according to the manufacturer's technical datasheets, with the mixing ratio of 4:1.

The samples were prepared by adding the hardener into the base resin in the recommended ratio followed by gently stirring the mix, with special care to avoid formation of air bubbles, until a homogenous mix was reached. The specimens were prepared and stored in laboratory (at 20˚C

and 60% RH) for two months before exposure to environmental conditions. The specimens prepared for HG exposure were cured for a longer period (three months) due to the unavailability of the climatic chamber.

2.2 Exposure conditions

The samples, after curing in the laboratory, were exposed to four environmental conditions according to Table 1. The exposure conditions consisted of real (outdoor) environmental conditions (OC), water immersion (WI), and hygrothermal conditions (HG). In order to provide a baseline, a set of control specimens was also kept in indoor laboratory conditions (IC) throughout the tests.

The real exposure (OC) consisted of placing the specimens in North of Portugal (Guimarães) in direct exposure to sun and rain (with the geographic coordinates of 41°27'06.9"N 8°17'32.8"W). The variations of temperature, relative humidity and rain content during the test period are shown in Fig 1. The specimens, after two months of curing, were exposed to 9 months in total with the post-ageing tests performed after 2, 4, 7 and 9 months.

The water immersion (WI) consisted of immersing the specimens in a water tank in a controlled environmental chamber room with 20°C and 60% R.H. The tank was filled with pure tab water having a pH in the range of 6.7-7.9 (with SO_4<10 mg/L, Mg<1 mg/L, Cl<10 µg/L and Ca=6 mg/L), according to the water supplier. The tank was periodically checked and changed with fresh water during the tests. The specimens, after two months curing, were immersed for a total of 9 months and were taken from the tank after 2, 4, 7 and 9 months for performing the tests.

The hygrothermal exposure (HG) consisted of exposing the samples to 6-hour temperature cycles (2 hrs at 10˚C, transition to 50˚C in 1 hr, 2 hrs at 50˚C, transition to 10˚C in 1 hr) with constant

relative humidity of 90%. The specimens were cured initially for three months, exposed to a total of 960 cycles and were taken from the climatic chamber every 240 cycles (corresponding to two months of exposure) for performing the DSC tests.

The specimens, after removal from the climatic chambers, were stored in controlled laboratory conditions for one week before performing the DSC tests. The water immersion (WI) and hygrothermal exposure (HG) tests were a replication of the conditions investigated by Maljaee et. al. [3,21] on the environmental degradation of bond in FRP-masonry systems.

2.3 Test procedures

2.3.1 Gravimetric measurement

The weight changes in the samples were measured to assess the moisture uptake during each exposure condition. Five specimens were periodically taken from the environment, wiped with a dry cloth and carefully weighed using digital balance with the accuracy of 0.01 gr. After the measurements, the samples were promptly placed again in the test conditions.

2.3.2 Calorimetric analysis

Several methods have been used in the literature for thermal characterization of polymers, such as Differential Scanning Calorimetry (DSC) and Dynamic Mechanical Analysis (DMA) [31,36,37]. Non-isothermal DSC tests were performed in this study to quantify the variation of T_g and relaxation enthalpy during each environmental exposure.

The samples were taken from the dog-bone shaped specimens using a specific cutter and weighed carefully with a high resolution digital balance (with accuracy of 0.001 mg). Three samples for each exposure period (10~14 mg) were tested using TA instruments (NETZSCH) DSC 200 F3 Maia. The samples were placed inside measuring pans, sealed, and then heated between 20˚C and 200˚C at a constant heating rate of 10˚C/min under nitrogen atmosphere. An

empty stainless sealed pan was also used as a reference inside the furnace. Attention was given in cutting the samples such that their shapes to be as regular as the bed of measuring pans.

In WI and HG-specimens, the DSC tests were performed in two scans. In this case, the samples, after heating up to 200˚C in the first scan, were cooled at the controlled rate of 10˚C/min down to 20˚C followed by reheating up to 200˚C with the same rate. The results obtained from the first heating, indeed, represents the effect of thermal history and curing of the sample, i.e. processing and ageing, on its thermal properties [38,39]. The inherent properties of the material (and the reversibility of the observed changes in the first scan) can be however observed in the second scan, as the thermal history and the physical ageing are eliminated during the first scan [40]. The objective was therefore to see if the specimens exposed to WI and HG conditions experienced any irreversible structural change.

2.4 Methodology and DSC curve interpretation

Interpretation of the DSC curves of the specimens exposed to different environmental conditions is a complex task as the curves are not usually clean and contain several artifacts. A clear understanding of the factors that lead to the observed artifacts is important in the analysis of the obtained results.

A virtual DSC curve containing all the observed characteristic regions is presented in Fig 2. It should be noted that this is a manipulated curve and thus not all the test results contained these artifacts together. In general, four key regions were identified in the results from the first heating scan: (1) a small endothermic peak occurred in some specimens before the relaxation enthalpy zone (in which the T_g occurs). The peak may be resulted due to settlement of the samples inside the sealed pan accompanied with heat absorption [41]. This artifact was removed from the curves before interpretation and analysis of the results; (2) the relaxation enthalpy peak in which the T_g

can be identified. This sub- T_g endothermic reaction can also represent the physical ageing in epoxy resins [42]; (3) some artifacts were observed in the third region that are probably due to the movement of sample inside the pan. These points can be neglected in the thermal interpretation as no weight loss was observed during the transition; (4) an exothermic reaction was observed at higher temperatures in some specimens. In cold-curing epoxies that are not fully cross-linked, such an exothermic peak has been reported in the literature and attributed to the residual cross-linking reaction and completion of curing [11,25,43,44]. This exothermic peak, which occurs at temperatures higher than T_g, diminished in the specimens cured for longer periods. The results from the second heating scan, generally, did not contain these artifacts as a natural consequence of elimination of the thermal history and physical aging of the specimens.

Among the outputs of non-isothermal DSC tests, several parameters are frequently presented and used (throughout this paper) such as the glass transition temperature (T_g), the relaxation peak (T_p) and its corresponding heat flow, and relaxation enthalpy (ΔH_{relax}).

T_g is defined as the temperature in which the polymer transforms from the glassy state to the rubbery state [45]. This transformation usually occurs in a temperature range rather than an exact temperature and its characterization is not always straightforward. Several methods have thus been proposed in the literature for obtaining the T_g from the DSC tests. The obtained results are consequently dependent on the adopted method in addition to the other influencing factors including heating/cooling rate [46]. The measurement conditions were thus kept constant throughout this study for logically comparing the results of different exposures. All the tests were conducted by applying thermal scans between 20˚C and 200˚C at a constant heating rate of 10˚C/min under nitrogen atmosphere.

As for identification of the T_g, the three characteristic temperatures proposed by ASTM E1356-08 [47] are considered here and the results are compared throughout the paper: (1) the extrapolated onset temperature, $T_{g(o)}$; (2) the midpoint temperature which occurs at the half-height of the heat capacity, $T_{g(m)}$; and (3) the inflection point temperature, $T_{g(i)}$.

The analysis of the results was performed by TA software (NETZSCH Proteus TA). For calculation of the T_g, it is important to accurately select the slope of the curves before and after the relaxation enthalpy. This is a challenging task in cases in which the curves contain several artifacts, see Fig 3. After selection of these two slopes, the T_g is automatically determined by TA software according to all three adopted methods.

The relaxation peak (T_p) is corresponding to the temperature in which the peak relaxation enthalpy occurs. The endothermic peak occurred after, but close to, the glass transition temperature and represents the physical ageing phenomenon. This increase in the heat capacity is due to the increase in required energy to initiate the molecular motions in rubbery phase. The position of endothermic peak and its intensity depends upon ageing conditions, i.e. temperature and time [48]. In current study, it was observed in the DSC curves that the endothermic peak tends to be centered at higher temperatures than T_g. This phenomenon which is also called as T_g overshoot, shows a high level of ageing in epoxy resin [22,49].

The relaxation enthalpy (ΔH_{relax}) is the area of endothermic peak over the baseline. A virtual baseline is thus required to be introduced to the DSC curves. The baseline connects the two points (before and after the relaxation enthalpy) over the DSC thermograph where the specimen is in a steady state with no transition or reactions occurring in the sample [50]. Several baseline types such as line, spline, and tangential baseline can be applied for this reason [51]. Among the available models, the 'Bezier' fitting method was chosen in this study.

3 Experimental results

3.1 Laboratory isothermal curing condition (IC)

The DSC curves of the IC samples are presented in Fig 4. The variation of T_p and the corresponding heat flow (denoted as peak heat flow in the figures) are also presented as the average of three tested specimens. The DSC tests were performed using a single heating scan (heated once between 20˚C-200˚C) after two, six and eleven months of isothermal curing condition. The results are used to investigate the changes in thermal behavior of epoxy in long-term isothermal conditions as well as for providing a baseline for other considered environmental conditions. The gravimetric measurements did not show any specific changes of weight in the specimens along the exposure period and thus the recorded changes in the thermal properties are solely related to curing time. It must be noticed that the moisture content of the specimens in unconditioned IC-specimens (reference specimens cured for two months) was assumed zero in the presented graph, see Figs 5, 7, 9, 12. The values presented for other exposure periods are therefore relative to these specimens.

The DSC curves, see Fig 4, show consistent increment of the T_p reaching about 15% increase after eleven months. The heat flow has increased in the first three months and then decreased until the end of the tests. The observed decrease in the heat flow intensity at peak can be attributed to the cross link density improvement in the specimens. DSC curves show that an exothermic peak has started at around 160˚C in the specimens cured for more than six months.

The changes of T_g and relaxation enthalpy, ΔH_{relax}, with curing time are presented in Fig 5. The predicted T_g values differ slightly with respect to the adopted method. While, $T_{g(m)}$ and $T_{g(i)}$ increased until the end of the tests, $T_{g(o)}$ seems to have reached a plateau after six months of curing, Fig 5a. The coefficient of variation (CoV) of the $T_{g(o)}$ and $T_{g(m)}$ are generally more than

$T_{g(i)}$ but all in an acceptable range. The sensitivity of the obtained T_g values and their variation with time to the adopted measurement method is clear in the obtained results. The incremental trend observed in T_g is a direct result of progress in cross-linking reactions through the time. It is well known that T_g can be used as an accurate indication of the cross-link density in epoxy resins [52]. As the curing continues, the cross-link density increases which is reflected in increment of T_g [53]. This increment until considerably long periods, in comparison to the short periods usually indicated in technical datasheets for complete curing of epoxy resins, has also been reported before for cold-curing epoxies [11,43]. This is due to the molecular conformation and reduction of free volume in long-term curing at room-temperature conditions.

The changes of relaxation enthalpy, ΔH_{rel}, with curing time are presented in Fig 5b. The relaxation enthalpy, which is a measure of physical aging, does not show any specific changes during the first six months and then decreases significantly until 11 months. This shows reduction of physical aging and increment of cross link density in the epoxy resin in the second half of the exposure period [22].

3.2 Effect of water immersion (WI)

The DSC curves of WI samples are shown in Fig 6 for both heating scans. The figure also shows how the enthalpy relaxation peak temperature and intensity (T_p and the heat flow) vary with immersion time. The tests were performed after two (one scan), four (one scan), seven (two scans) and nine (two scans) months of immersion. It can be observed that T_p decreases (about 6%) until seven months and then it increases afterwards. This observation is in contrary to the IC specimens in which increment of T_p with curing time was observed in the specimens. On the other hand, the heat flow at relaxation peak, besides some fluctuations, seems constant until

seven months followed by a decrement afterwards. It seems that the long-term water immersion (after seven months) has induced a contrary effect on T_p and peak heat flow intensity.

The thermal behavior of WI samples after the endothermic region is also interesting. It seems the exothermic reaction, which was observed in IC specimens at temperatures higher than 160˚C, has slightly shifted to lower temperatures, see Fig 6.

The changes of T_g in the first and the second scans, together with the moisture content, are shown in Fig 7a-b. The variation of the results was in an acceptable range with the largest CoV=9%. The specimens absorbed 2.05% mass water at the end of the exposure period and it seems that the saturation level was not yet reached. Although the absolute values of T_g are slightly different for $T_{g(o)}$, $T_{g(i)}$ and $T_{g(m)}$, it seems that the general trend of its changes is similar in all adopted models. The first scan's T_g slightly decreases with time (and water absorption) until seven months and then it increases afterwards, see Fig 7a. In the first scan of DSC test, the sample was heated up to far above the T_g and consequently its thermal history was eliminated. The specimens are then fully cured during the cooling process. By elimination of all the reversible effects of physical ageing and curing of the epoxy resin in the second scan, the T_g stands on a higher value compared to T_{g1}. The increment of T_{g2} until the end of exposure period, see Fig 7b, is an indication of chemical changes in the structure of epoxy resin in this environment. This value increased up to 8% by the end of WI exposure.

In the presence of moisture, two major mechanisms (namely plasticization and hydrolysis) can become activated leading to decrement of T_g [29]. Plasticization is a physical ageing process and possesses a reversible effect on the epoxy resin. On the other hand, hydrolysis is a chemical aging process and can change the chemical structure of the epoxy resin irreversibly. Exposure to long-term moisture conditions can also lead to post-curing (also a chemical mechanism) of

epoxy resins and thus increment of T_g [54], as explained before. The chemical changes of epoxies can be distinguished in the DSC results obtained from the second heating scan (T_{g2}) [40], as also explained in the last sections. The combination of all the above mentioned mechanisms has led to the observed changes in the T_g, presented in Fig 7. The initial decrement of T_{g1}, shows the larger contribution of plasticization and hydrolysis in this period, see Fig 7a. Meanwhile, the increment of T_{g2} at the end of WI exposure can be associated to the larger contribution of post-curing [55,56].

The enthalpy relaxation shows large variations and fluctuations with immersion time, see Fig 7c. The general trend, however, seems to be slightly downwards.

3.3 Effect of hygrothermal exposure (HG)

The DSC curves of HG specimens in both heating scans together with the variation of enthalpy relaxation peak temperature and heat flow are shown in Fig 8. Interesting changes can be observed in the thermal behavior of epoxy resin due to exposure to hygrothermal conditions. The exposure has led to a shift of T_p towards higher temperatures (total 24% increase after 960 cycles) and to decrement of its peak intensity heat flow (about 40% reduction in total). It can be observed that the first two months of exposure induced the largest changes in the thermal properties.

The changes in T_g and relaxation enthalpy of the specimens are presented in Fig 9. The results from the first heating scan show that the T_g changes with a slightly different trend in $T_{g(m)}$ and $T_{g(i)}$ in comparison to $T_{g(o)}$. While it seems that $T_{g(m)}$ and $T_{g(i)}$ have reached a plateau after the initial increment in the first two months of exposure, $T_{g(o)}$ shows a slight decrement in this period. The T_g from the second heating scans, however, follows a similar trend in all methods by increasing in the first two months and then stabilizing until the end of the tests.

The observed changes in the T_g are the result of several counteracting and interlinked mechanisms which affect the network structure of the epoxy resin. As observed in the WI specimens, moisture absorption causes plasticization in epoxy resin and thus leads to reduction of T_g. However, long-term exposure can change the trend and lead to increment of T_g. On the other hand, the epoxy is exposed to temperatures above its curing temperature (23˚C) and near its T_g during the hygrothermal exposure (when the temperature rises to 50˚C). This leads to further cross-linking and post-curing of epoxy and thus increment of T_g [56,57].

The changes of relaxation enthalpy are also illustrated in Fig 9c. A significant decrement of enthalpy has occurred during the first four months of exposure. This, which can be directly correlated to reduction of intensity of relaxation peak in DSC thermographs, is an evidence of progress in the cross-link density in the specimens due to post-curing. Post-curing, as a chemical reaction, is the responsible for the observed development of T_{g2}, see Fig 9b.

A comparison between T_{g2} in WI and HG conditions, Fig 10, shows while the post-curing of epoxy resin was advancing after 9 months of water immersion, the HG-specimens reached the $T_{g\infty}$ (about 76˚C) after only two months of exposure.

3.4 Effect of outdoor curing (OC)

The DSC curves together with changes of T_p and heat flow at peak relaxation in OC-specimens are shown Fig 11. The thermal behavior of OC-specimens did not change significantly during the exposure. Besides some slight fluctuations, no specific changes is observed in T_p and heat flow at peak intensity. Only a 26% decrease can be observed in the heat flow after nine months of exposure.

The T_g of the samples, presented in Fig 12a, does not also show specific changes with exposure time. Although, again, there is a sight difference in the T_g obtained from different methods.

Again, $T_{g(i)}$ and $T_{g(m)}$ have the largest and smallest values, respectively. It can be observed that the absorbed moisture is less in these specimens in comparison to HG- or WI-specimens. An incremental moisture content is observed until four months of exposure (reaching less than 1%) and then the trend is reversed until the end. This reversal trend in the moisture level is due to reduction of rain content and relative humidity along this period, see Fig 1.

The variation of relaxation enthalpy is presented in Fig 12b. In general, 65% increase in the enthalpy is observed until four months of exposure (an evidence of physical aging), and then the values are dropped. During the OC exposure, the specimens are subjected to several environmental factors such as humidity, solar Ultraviolet (UV) light, heat and chemical components, which can intrinsically lead to degradation in polymeric materials [38]. The obtained results are therefore a combination of these counteracting effects.

4 Effect of moisture absorption

The changes of moisture content and T_g of the specimens in different exposure conditions are compared in Fig 13. It can be observed that the WI and HG specimens have reached a similar amount of moisture level at the end of exposure period. HG specimens show a higher rate of moisture absorption during the first months which can be due to exposure to higher temperatures in this condition. The specimens exposed to real exposure conditions (OC) have absorbed the lowest amount of moisture during the tests period. Both WI and HG conditions seem to significantly increase the rate of water absorption in comparison to real exposure conditions (in the selected region and in the studied period). The results related to IC specimens are not presented here as the specimens did not show any specific change of weight.

A look at the changes of T_g, Fig 13(b), shows the HG specimens experienced an improvement in cross-link density during the exposure. Although the HG specimens have a similar moisture

absorption as WI specimens, it seems that the post-curing mechanism have governed the moisture-induced plasticization leading to improvement of T_g. IC specimens also show an improvement of cross-link density, but smaller than HG, until the end of exposure.

The results from the WI tests can be used for correlating the changes of T_g with moisture absorption (neglecting the effect of natural aging time). It was assumed that a quadratic equation, as also used in [58], can be used to correlate the variation of glass transition temperature with the moisture absorption:

$$T_{gw}/T_{gd}=A\omega^2-B\omega+C \quad (1)$$

where T_{gw}, T_{gd} are T_g in wet and dry states, respectively, ω is the percentage of moisture content and A, B, C are the constants. These constants can be obtained by fitting the experimental results of WI specimens (see Fig 14a) leading to the following relation:

$$T_{gw}/T_{gd}=0.06\omega^2-0.14\omega+1 \quad (2)$$

As the water immersion tests were performed in controlled temperature conditions, it is expected that the obtained changes of glass transition temperature are solely related to water absorption in combination with the contrary effect of curing time (or natural aging of the specimens). As explained in the last sections, partially-cured epoxy resins under moisture conditions, are contemporary subjected to different complex processes such as continuation of cure as a chemical process, plasticization as a physical aging process, and hydrolysis and post-curing (in long-term periods) as chemical aging processes. Although the water-induced changes (plasticization, hydrolysis, post-curing, etc.) can be related to moisture absorption level (as also previously done in the literature), the effect of time (natural aging) should be considered separately. As in the experimental data presented in this study the effect of natural curing is not

isolated from water induced degradation processes, Eq (2) is not applicable to other sets of data and is solely presented for comparison with other exposure conditions investigated here.

Application of Eq (2) to the results obtained from HG and OC conditions (having the moisture absorption level in each condition) helps in isolating the effect of moisture level (and curing time) from other active mechanisms (temperature cycles, sun, etc.), see Fig 14(b, c). It should be noted that the T_g values are normalized to their reference values so that comparison can be done between different environmental conditions. The changes of T_g in IC-conditions are also presented in the figures as the baseline.

Fig 14(b) shows the expected reduction of T_g with moisture absorption in HG conditions. The difference of predicted values with experimental ones can be attributed to the post-curing effects [11,27]. A comparison between the changes of T_g in OC and HG specimens, shows probably the HG exposure studied here is not the best replicating condition for the studied region and is possibly more suitable in warmer areas in which post-curing effects can be more pronounced. It should however be noted that this comparison is made between long-term accelerated aging tests and extremely short real exposure periods which can be another reason for the observed differences.

Fig 14(c) shows the expected depression of T_g with exposure time due to moisture absorption in OC conditions. It seems that Eq. (2) can predict the changes of T_g in real exposure conditions (OC) with an acceptable degree of accuracy. This is the evidence of the fact that in OC conditions considered in this study, the governing aging mechanism has been moisture absorption and curing time although other existing degradation mechanisms, such as UV exposure and temperature variations, concurrently exist.

5 Conclusion

This study focused on the influence of long-term environmental conditions on the thermal behavior of a typical epoxy resin used for externally bonded reinforcement of masonry structures through DSC tests. Four different environmental conditions including water immersion, accelerated hygrothermal exposure, outdoor exposure and indoor laboratory conditions were considered. Three conventional characteristic temperatures (onset, midpoint and inflection point) were considered for calculating the glass transition temperature, T_g, and the sensitivity of the results to the adopted method was investigated. The following conclusions can be drawn from the experimental observations:

- Using different characteristic temperatures, a wide range of T_g values and in some cases different degradation trends were observed, which can affect the interpretation of the experimental results.
- The T_g of epoxy resin increased 12% after eleven months of curing in laboratory conditions. This observation is contradictory to the short periods suggested in the technical datasheets for complete curing of epoxy resins. These changes should be considered in interpretation of the experimental results and at the design stage as usually the measurements are conducted at relatively early ages (e.g. 2 months).
- Water immersion (WI) led to a reduction of T_g with moisture absorption level. Cyclic DSC tests showed that a significant portion of the observed depression was reversible. An increase of T_g was observed after seven months of immersion which was attributed to the contradictory effect of water absorption in long-term periods.
- Hygrothermal conditions (HG) led to increment of glass transition temperature. This observation was due to the fact that post-curing of epoxy resin governed the plasticization effect

of moisture in these specimens. The increment of T_g was in contrary to the observed changes in the specimens exposed to outdoor conditions, showing that possibly the considered hygrothermal conditions was not the most suitable for predicting the real conditions in this region. It should be however noted that the comparisons were made between relatively long-term accelerated aging tests and extremely short real exposure tests (1 year) which can be another reason for the observed differences.

- An analytical model was developed for correlating the changes of T_g with moisture absorption level. The developed model was then used for investigating the effect of moisture absorption in hygrothermal and outdoor exposure tests. It was observed that the changes of T_g in the specimens exposed to outdoor conditions can be accurately predicted with the developed analytical model.
- The impact of moisture on the glass transition temperature of epoxy resins is a complex phenomenon. Complementary tests such as FTIR (Fourier transform infrared spectroscopy), TGA (thermal gravimetric analysis) and MDSC (Modulated DSC) are recommended for better understanding the degradation mechanisms. Since epoxy resin is a non-crystalline polymer, performing the DSC tests with a wider temperature range will not give us important information, while, starting tests from lower temperature ranges (<20˚C), seems interesting particularly in the specimens exposed to moist environments.

Acknowledgements

The second author acknowledges the financial support of the Ministério da Ciência, Tecnologia e Ensino Superior, FCT, Portugal, under the grant SFRH/BPD/92614/2013 as well as the financial support of the European Union's Marie Curie Individual Fellowship program under REA grant

agreement No. 701531. This work was partly financed by FEDER funds through the Competitively Factors Operational Programme - COMPETE and by national funds through FCT – Foundation for Science and Technology within the scope of the project POCI-01-0145-FEDER-007633.

References

[1] Karbhari VM, Chin JW, Hunston D, Benmokrane B, Juska T, Morgan R, et al. Durability gap analysis for Fiber-Reinforced Polymer composites in civil infrastructure. J Compos Constr 2003;7(3):238–47.

[2] Maxwell AS, Broughton WR, Dean G, Sims GD. Review of accelerated ageing methods and lifetime prediction techniques for polymeric materials. NPL Rep DEPC MPR 016 2005.

[3] Maljaee H, Ghiassi B, Lourenço PB, Oliveira DV. FRP–brick masonry bond degradation under hygrothermal conditions. Compos Struct 2016;147:143–54.

[4] Ghiassi B, Marcari G, Oliveira DV, Lourenço PB. Water degrading effects on the bond behavior in FRP-strengthened masonry. Compos Part B Eng 2013;54:11–9.

[5] Karbhari VM, editor. Durability of composites for civil structural applications, Cambridge, England: Woodland; 2007.

[6] Karbhari VM, Abanilla MA. Design factors, reliability, and durability prediction of wet layup carbon/epoxy used in external strengthening. Compos Part B Eng 2007;38(1):10–23.

[7] Abanilla MA, Li Y, Karbhari VM. Durability characterization of wet layup graphite/epoxy composites used in external strengthening. Compos Part B Eng 2005;37(2–3):200–12.

[8] Guermazi N, Ben Tarjem A, Ksouri I, Ayedi HF. On the durability of FRP composites for aircraft structures in hygrothermal conditioning. Compos Part B Eng 2013;85:294–304.

[9] Blackburn BP, Tatar J, Douglas EP, Hamilton HR. Effects of hygrothermal conditioning on epoxy adhesives used in FRP composites. Constr Build Mater 2015;96:679–89.

[10] Moussa O, Vassilopoulos AP, Keller T. Effects of low-temperature curing on physical behavior of cold-curing epoxy adhesives in bridge construction. Int J Adhes Adhes 2012;32(1):15–22.

[11] Lettieri M, Frigione M. Effects of humid environment on thermal and mechanical properties of a cold-curing structural epoxy adhesive. Constr Build Mater 2012;30:753–60.

[12] Hu Y, Li X, Lang AW, Zhang Y, Nutt SR. Water immersion aging of polydicyclopentadiene resin and glass fiber composites. Polym Degrad Stab 2016;124:35–42.

[13] Hu Y, Lang AW, Li X, Nutt SR. Hygrothermal aging effects on fatigue of glass fiber/polydicyclopentadiene composites. Polym Degrad Stab 2014;110:464–72.

[14] Banhegyi G, Vargha V, Muller P, Zelenyanszki E. Estimation of thermal acceleration factors of ageing epoxy insulation using thermogravimetry and intuitive kinetic model. IEEE Trans Dielectr Electr Insul 2009;16(5):1420–9.

[15] Islam MS, Tong L. Effects of hygrothermal and ambient humidity conditioning on shear strength of metal-GFRP single lap joints co-cured in and out of water. Int J Adhes Adhes 2016;68:305–16.

[16] Jiang X, Qiang X, Kolstein MH, Bijlaard FSK. Experimental investigation on mechanical behaviour of FRP-to-steel adhesively-bonded joint under combined loading - Part 2: After

hygrothermal ageing. Compos Struct 2015;125:687–97.

[17] Yang Q, Xian G, Karbhari VM. Hygrothermal ageing of an epoxy adhesive used in FRP strengthening of concrete. J Appl Polym Sci 2007;107:2607–17.

[18] Zheng XH, Huang PY, Chen GM, Tan XM. Fatigue behavior of FRP-concrete bond under hygrothermal environment. Constr Build Mater 2015;95:898–909.

[19] Benzarti K, Chataigner S, Quiertant M, Marty C, Aubagnac C. Accelerated ageing behaviour of the adhesive bond between concrete specimens and CFRP overlays. Constr Build Mater 2011;25(2):523–38.

[20] Ghiassi B, Lourenço PB, Oliveira DV. Accelerated hygrothermal aging of bond in FRP–masonry systems. J Compos Constr 2015;19(3):4014051.

[21] Maljaee H, Ghiassi B, Lourenço PB, Oliveira DV. Moisture-induced degradation of interfacial bond in FRP-strengthened masonry. Compos Part B Eng 2016;87:47–58.

[22] Odegard GM, Bandyopadhyay A. Physical aging of epoxy polymers and their composites. J Polym Sci Part B Polym Phys 2011;49(24):1695–716.

[23] Montserrat S. Vitrification and physical ageing on isothermal curing of an epoxy resin. J Therm Anal 1991;37(8):1751–8.

[24] Plazek DJ, Frund ZN. Epoxy resins (DGEBA): The curing and physical aging process. J Polym Sci Part B Polym Phys 1990;28(4):431–48.

[25] Frigione M, Naddeo C, Acierno D. Cold-curing epoxy resins: aging and environmental effects. I-Thermal properties. J Polym Eng 2001;21(1):23–52.

[26] Carbas RJC, da Silva LFM, Marques EAS, Lopes AM. Effect of post-cure on the glass transition temperature and mechanical properties of epoxy adhesives. J Adhes Sci Technol 2013;27(23):2542–57.

[27] Perrin FX, Nguyen MH, Vernet JL. Water transport in epoxy-aliphatic amine networks - Influence of curing cycles. Eur Polym J 2009;45(5):1524–34.

[28] Deroin M, Le Duigou A, Corre YM, Le Gac PY, Davies P, Cesar G, et al. Accelerated ageing of polylactide in aqueous environments: Comparative study between distilled water and seawater. Polym Degrad Stab 2014;108:319–29.

[29] Ghorbel I, Valentin D. Hydrothermal effects on the physico-chemical properties of pure and glass fiber reinforced polyester and vinylester resins. Polym Compos 1993;14(4):324–334.

[30] Wu C-S. Influence of post-curing and temperature effects on bulk density , glass transition and stress-strain behaviour of imidazole-cured epoxy network. J Mater Sci 1992;27:2952–9.

[31] Michels J, Widmann R, Czaderski C, Allahvirdizadeh R, Motavalli M. Glass transition evaluation of commercially available epoxy resins used for civil engineering applications. Compos Part B Eng 2015;77:484–93.

[32] Czaderski C, Martinelli E, Michels J, Motavalli M. Effect of curing conditions on strength development in an epoxy resin for structural strengthening. Compos Part B Eng 2012;43(2):398–410.

[33] Stewart I, Chambers A, Gordon T. The cohesive mechanical properties of a toughened epoxy adhesive as a function of cure level 2007;27:277–87.

[34] Bao L-R, Yee AF. Effect of temperature on moisture absorption in a bismaleimide resin and its carbon fiber composites. Polymer (Guildf) 2002;43(14):3987–97.

[35] Hollaway LC. A review of the present and future utilisation of FRP composites in the civil infrastructure with reference to their important in-service properties. Constr Build Mater

2010;24(12):2419–45.

[36] He Y, Fan Z, Hu Y, Wu T, Wei J, Li S. DSC analysis of isothermal melt-crystallization, glass transition and melting behavior of poly(l-lactide) with different molecular weights. Eur Polym J 2007;43(10):4431–9.

[37] Moussa O, Vassilopoulos AP, Keller T. Experimental DSC-based method to determine glass transition temperature during curing of structural adhesives. Constr Build Mater 2012;28(1):263–8.

[38] Sharma KS, Mudhoo A, editors. A handbook of applied biopolymer technology: synthesis, degradation and application. Royal Society of Chemistry (RSC); 2011.

[39] Bengoechea C, Arrachid A, Guerrero A, Hill SE, Mitchell JR. Relationship between the glass transition temperature and the melt flow behavior for gluten, casein and soya. J Cereal Sci 2007;45(3):275–84.

[40] Soenen H, Besamusca J, Poulikakos LD, Planche J-P, Das PK, Kringos N, et al. Differential Scanning Calorimetry Applied to Bitumen: Results of the RILEM NBM TG1 Round Robin Test. In: Kringos N, Birgisson B, Frost D, Wang L, editors. Proc. Int. RILEM Symp., Stockholm, June 2013: Springer; 2013, p. 311–23.

[41] Shawe J, Riesen R, Widmann J, Schubnell M. UserCom 11. Mettler Toledo 2000;

[42] Drozdov AD. Physical aging in amorphous polymers: comparison of observations in calorimetric and mechanical tests. Eur Polym J 2001;37(7):1379–89.

[43] Corcione C, Freuli F, Frigione M. Cold-curing structural epoxy resins: analysis of the curing reaction as a function of curing time and thickness. Materials (Basel) 2014;7:6832–42.

[44] Hardis R, Jessop JLP, Peters FE, Kessler MR. Cure kinetics characterization and

monitoring of an epoxy resin using DSC, Raman spectroscopy, and DEA. Compos Part A Appl Sci Manuf 2013;49:100–8.

[45] Groenewoud VM. Characterization of polymers by thermal analysis. vol. 1. Cambridge: 2001.

[46] Hammer A. Thermal analysis of polymers. Mettler-Toledo 2013.

[47] ASTM E1356-08. Standard test method for assignment of the Glass Transition Temperatures by Differential Scanning Calorimetry 2014.

[48] Fraga F, Castro-Diaz C, Rodríguez-Núñez E, Martínez-Ageitos JM. Physical aging for an epoxy network diglycidyl ether of bisphenol A/m-xylylenediamine. Polymer (Guildf) 2003;44(19):5779–84.

[49] Chung HJ, Lee EJ, Lim ST. Comparison in glass transition and enthalpy relaxation between native and gelatinized rice starches. Carbohydr Polym 2002;48(3):287–98.

[50] Hohne GWH, Hemminger WF, Flammersheim HJ. Differential Scanning Calorimetry. vol. 84. 2nd editio. Hoboken, NJ, USA: John Wiley & Sons, Inc.; 2003.

[51] Haque MK, Kawai K, Suzuki T. Glass transition and enthalpy relaxation of amorphous lactose glass. Carbohydr Res 2006;341(11):1884–9.

[52] Simon SL, Mckenna GB, Sindt O. Modeling the evolution of the dynamic mechanical properties of a commercial epoxy during cure after gelation. J Appl Polym Sci 2000;76(4):495–508.

[53] Moussa O, Vassilopoulos AP, Castro J De, Keller T. Long-term development of thermophysical and mechanical properties of cold-curing structural adhesives due to post-curing. J Appl Polym Sci 2013;127(4):2490–6.

[54] Apicella A, Migliaresi C, Nicolais L, Laccarino L, Roccotelli S. The water ageing of

unsaturated polyester-based composites: influence of resin chemical structure. Composites 1983;14(4):387–92.

[55] Kutz M. Handbook of Environmental Degradation of Materials. William Andrew; 2012.

[56] Wondraczek K, Adams J, Fuhrmann J. Effect of thermal degradation on glass transition temperature of PMMA. Macromol Chem Phys 2004;205(14):1858–62.

[57] Zhou J, Lucas JP. Hygrothermal effects of epoxy resin. Part II: variations of glass transition temperature. Polymer (Guildf) 1999;40(20):5513–22.

[58] Chamis CC, Murthy PLN. Simplified adhesively procedures for designing bonded composite joints. J Reinf Plast Compos 1991;10:29–41.

List of Figures

Fig 1. Outdoor exposure environmental conditions. Variations of: (a) temperature; (b) relative humidity; (c) rain.

Fig 2. Virtual DSC curve.

Fig 3: The sequence of zooming process.

Fig 4. (a) DSC curves of IC-specimens (b) changes of T_p and corresponding heat flow.

Fig 5. Variation of (a) T_g (b) relaxation enthalpy in IC specimens (MC=moisture content).

Fig 6. (a) DSC curves of WI-specimens (b) changes of T_p and corresponding heat flow.

Fig 7. Variation of (a) T_g in the first scan; (b) T_g in the second scan and (c) relaxation enthalpy in WI-specimens (MC=moisture content).

Fig 8. (a) DSC curves of HG-specimens (b) changes of T_p and corresponding heat flow.

Fig 9. Variation of (a) first T_g (b) second T_g (c) relaxation enthalpy in HG-specimens (MC=moisture content).

Fig 10. Variation of T_{g2} in WI and HG-specimens.

Fig 11. (a) DSC curves of OC-specimens (b) changes of T_p and corresponding heat flow.

Fig 12. Variation of (a) T_g (b) enthalpy in OC-specimens (MC=moisture content).

Fig 13. Changes of (a) moisture absorption and (b) T_g in different environmental conditions.

Fig 14. Changes of T_{g1} with moisture absorption in (a) WI; (b) HG; (c) OC specimens.

List of Tables

Table 1. Tests program. 30

Table 1. Tests program.

Exposure	Condition	Total exposure time (months)	Test interval (months)	No. of thermal scans
IC (indoor laboratory condition)	20-23°C, 60% R.H.	11	3-6-11	1
OC (outdoor exposure condition)	Variable along time	9	2-4-7-9	1
WI (water immersion)	20-23°C, immersed	9	2-4-7-9	2
HG (hygrothermal conditions)	10-50°C, 90% R.H.	8	2-4-8	2

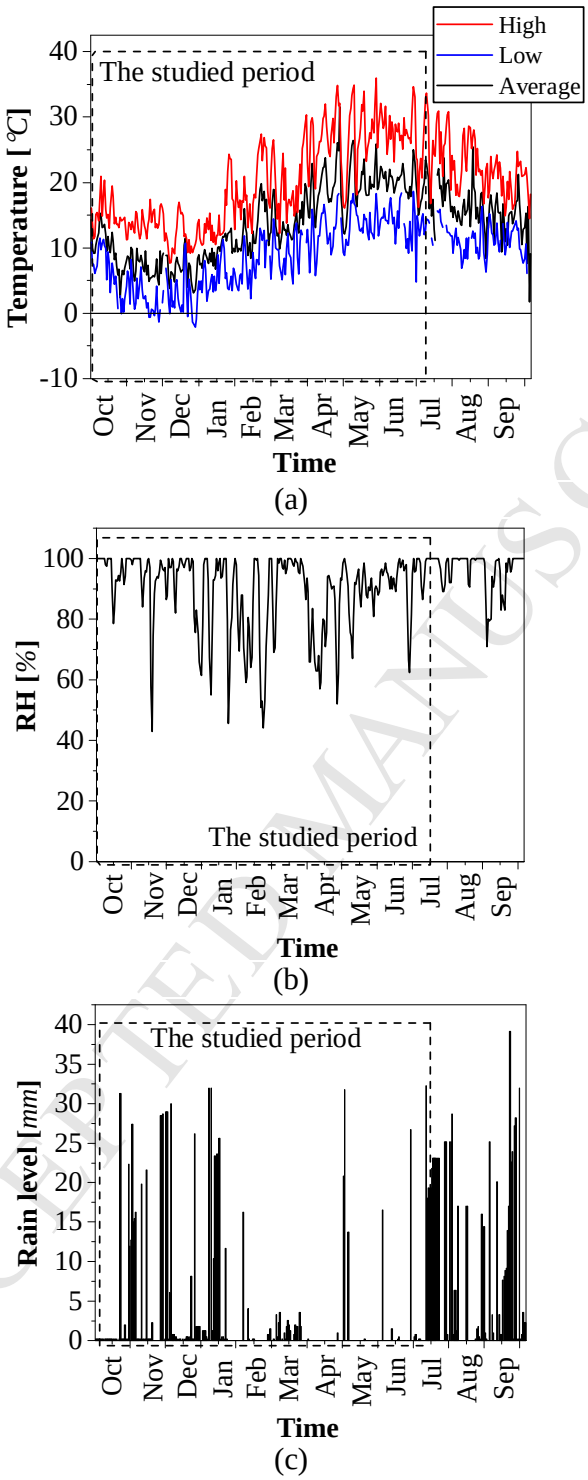

Fig 1. Outdoor exposure environmental conditions. Variations of: (a) temperature; (b) relative humidity; (c) rain.

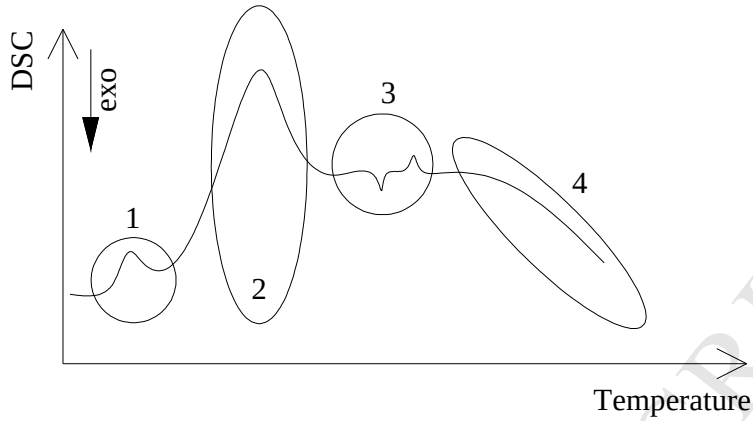

Fig 2. Virtual DSC curve.

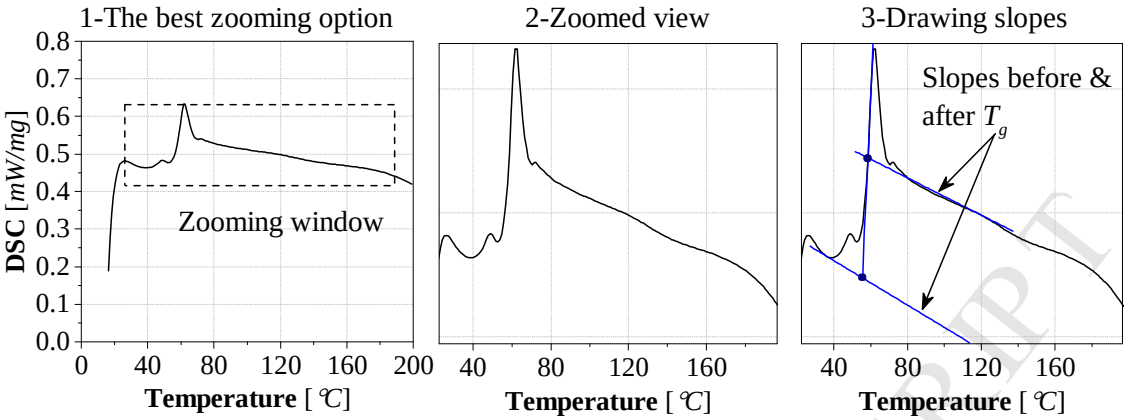

Fig 3: The sequence of zooming process.

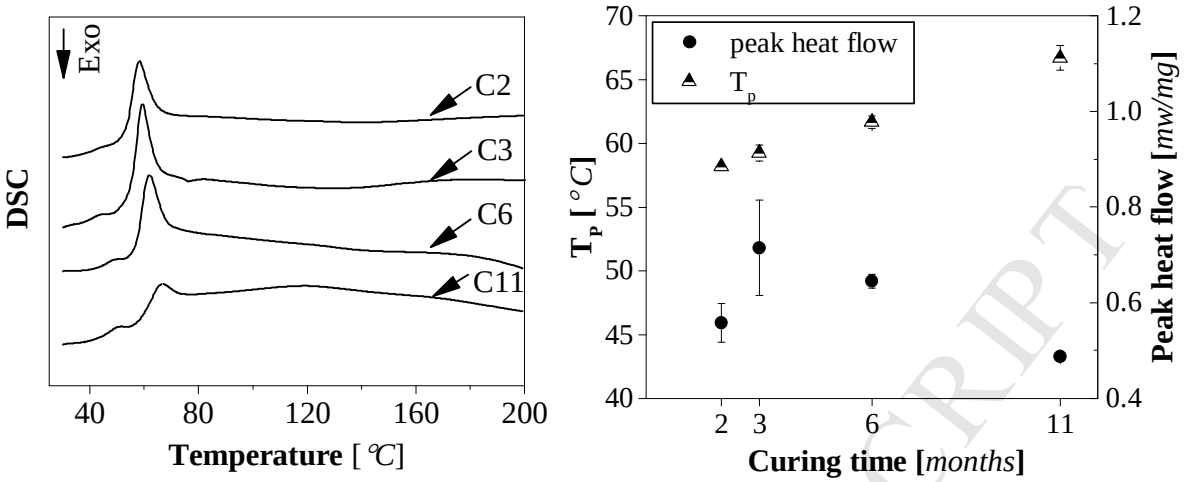

(a) (b)

Fig 4. (a) DSC curves of IC-specimens (b) changes of T_p and corresponding heat flow.

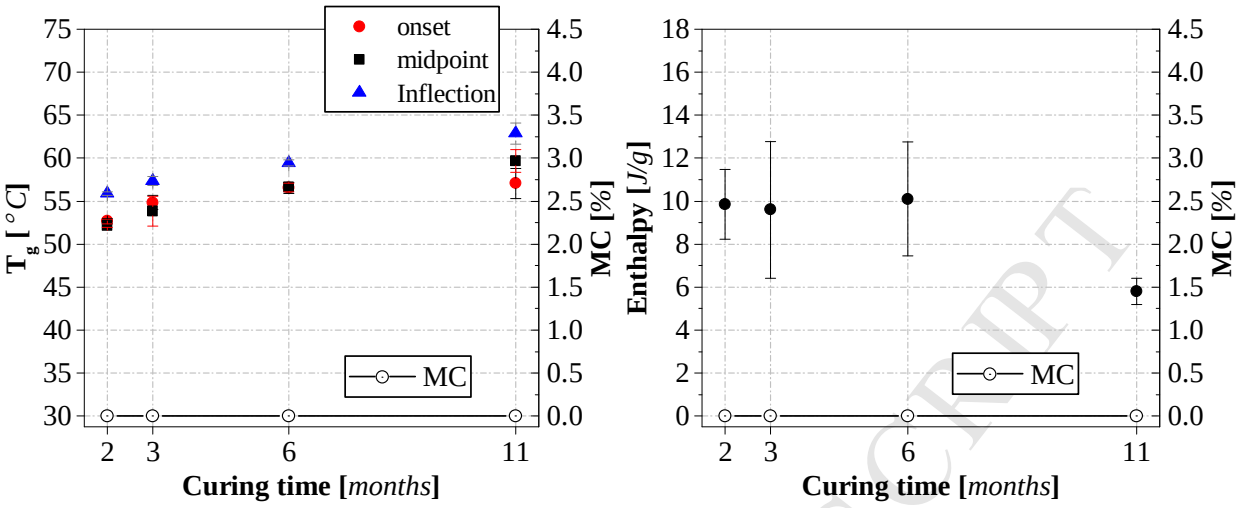

(a) (b)

Fig 5. Variation of (a) T_g (b) relaxation enthalpy in IC specimens (MC=moisture content).

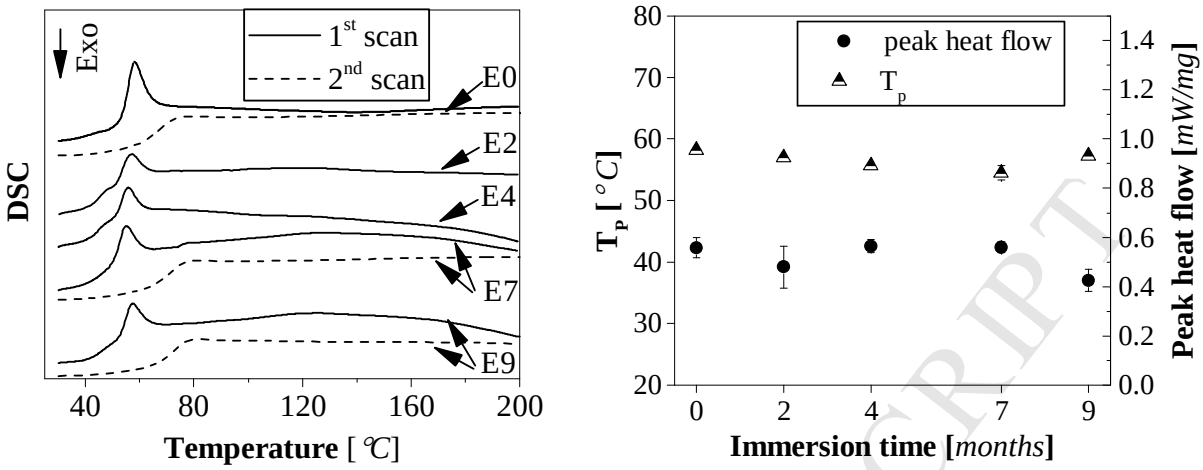

(a) (b)

Fig 6. (a) DSC curves of WI-specimens (b) changes of T_p and corresponding heat flow.

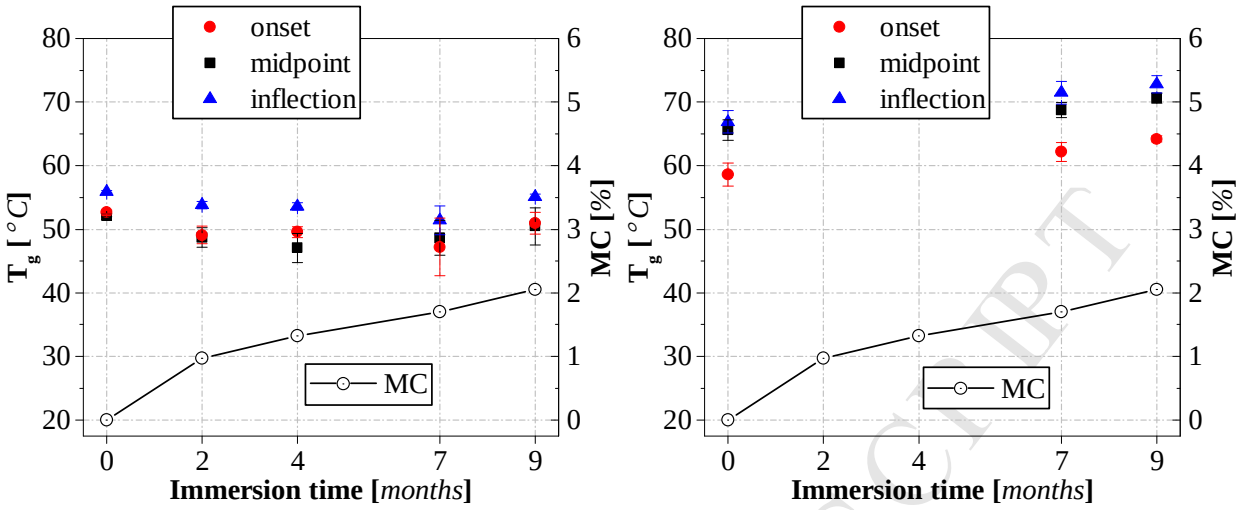

(a) (b)

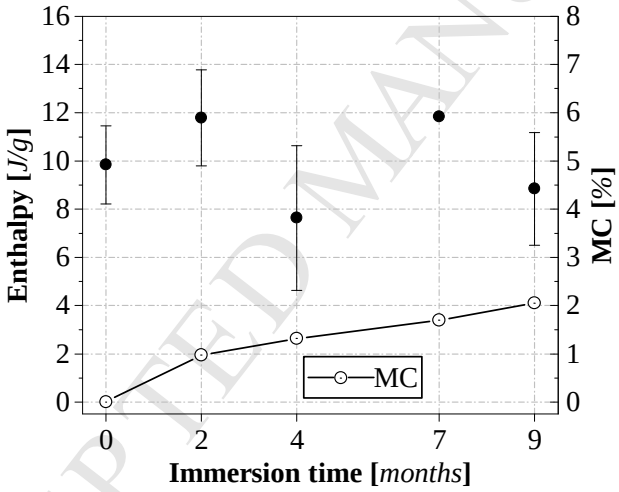

(c)

Fig 7. Variation of (a) T_g in the first scan; (b) T_g in the second scan and (c) relaxation enthalpy in WI-specimens (MC=moisture content).

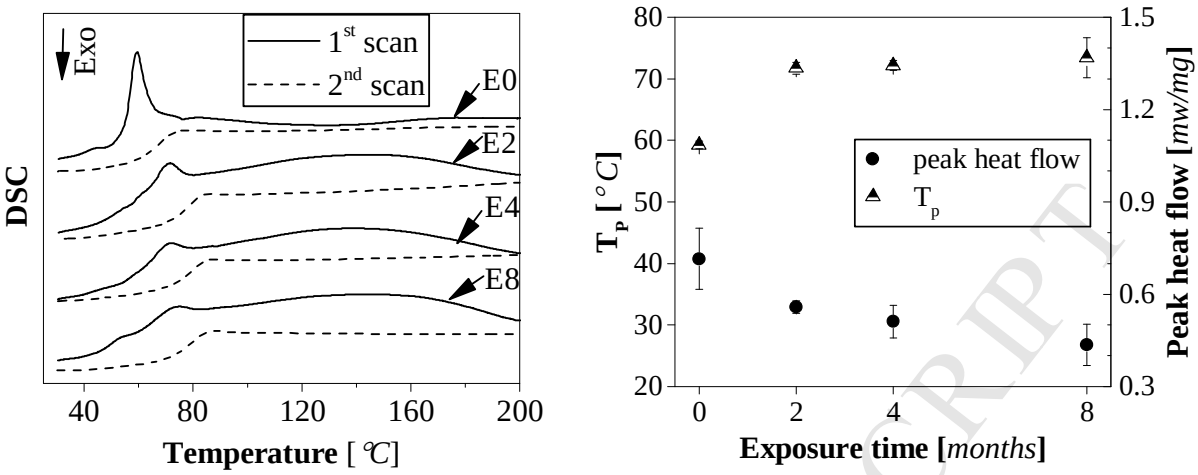

(a) (b)

Fig 8. (a) DSC curves of HG-specimens (b) changes of T_p and corresponding heat flow.

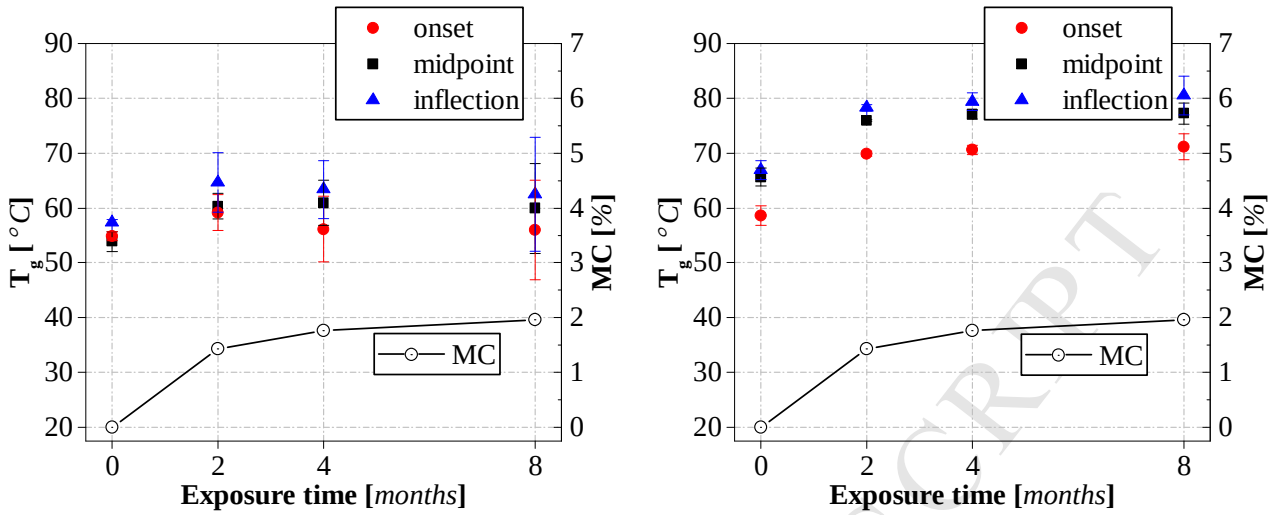

(a) (b)

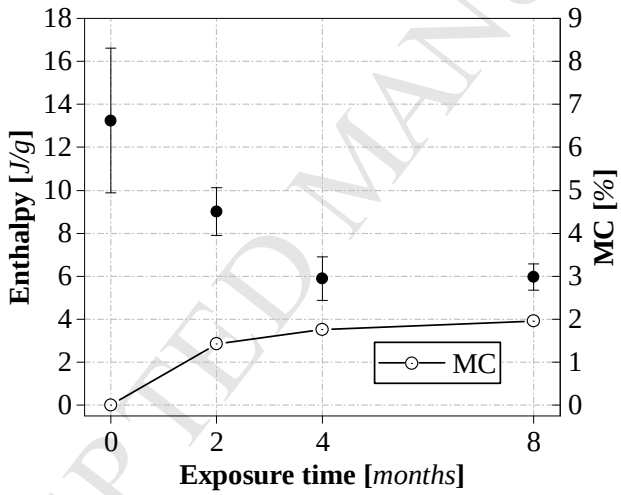

(c)

Fig 9. Variation of (a) first T_g (b) second T_g (c) relaxation enthalpy in HG-specimens (MC=moisture content).

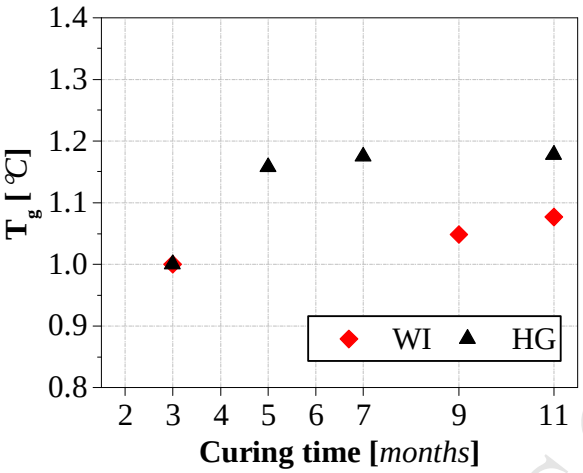

Fig 10. Variation of T_{g2} in WI and HG-specimens.

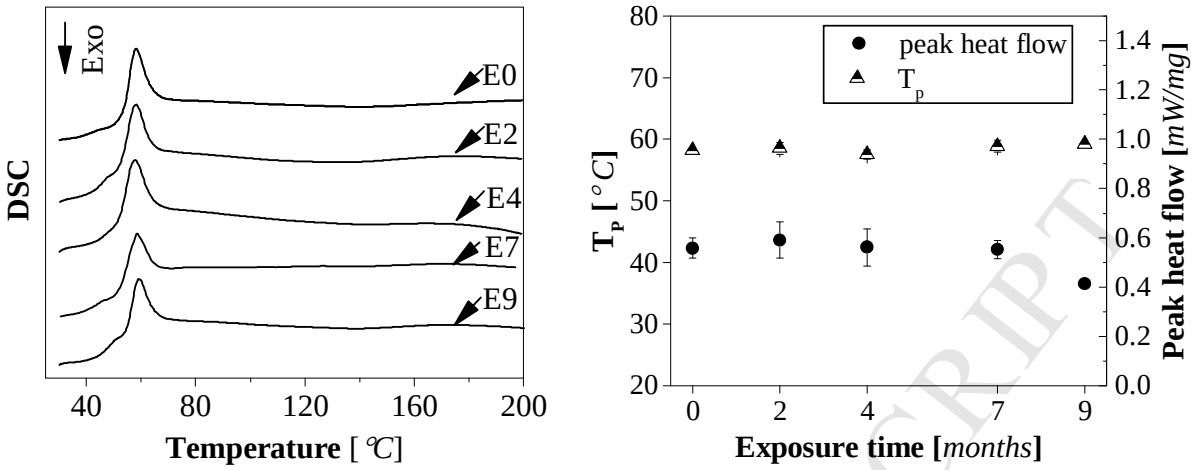

(a) (b)

Fig 11. (a) DSC curves of OC-specimens (b) changes of T_p and corresponding heat flow.

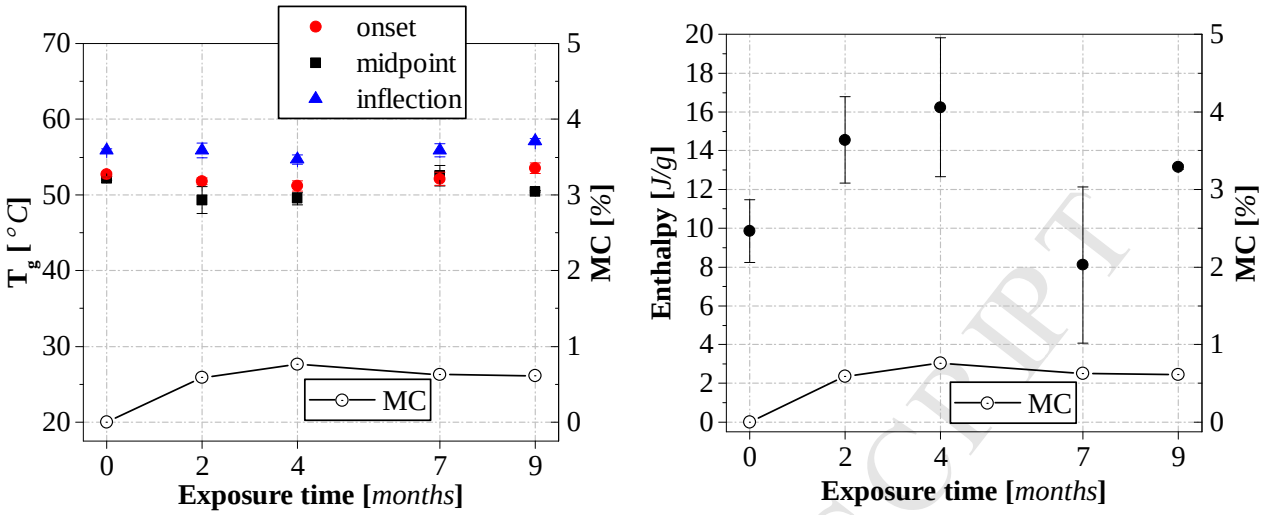

(a) (b)

Fig 12. Variation of (a) T_g (b) enthalpy in OC-specimens (MC=moisture content).

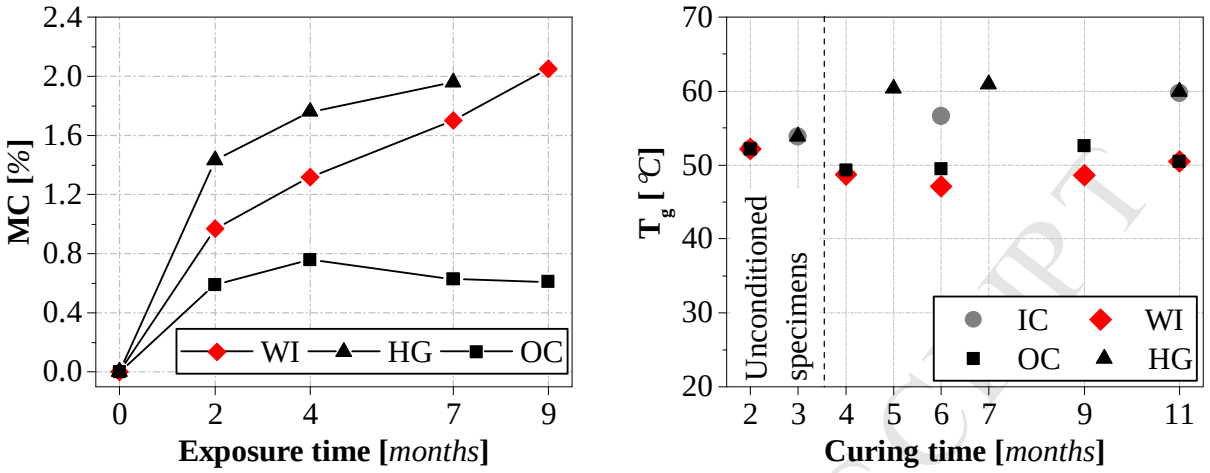

(a) (b)

Fig 13. Changes of (a) moisture absorption and (b) T_g in different environmental conditions.

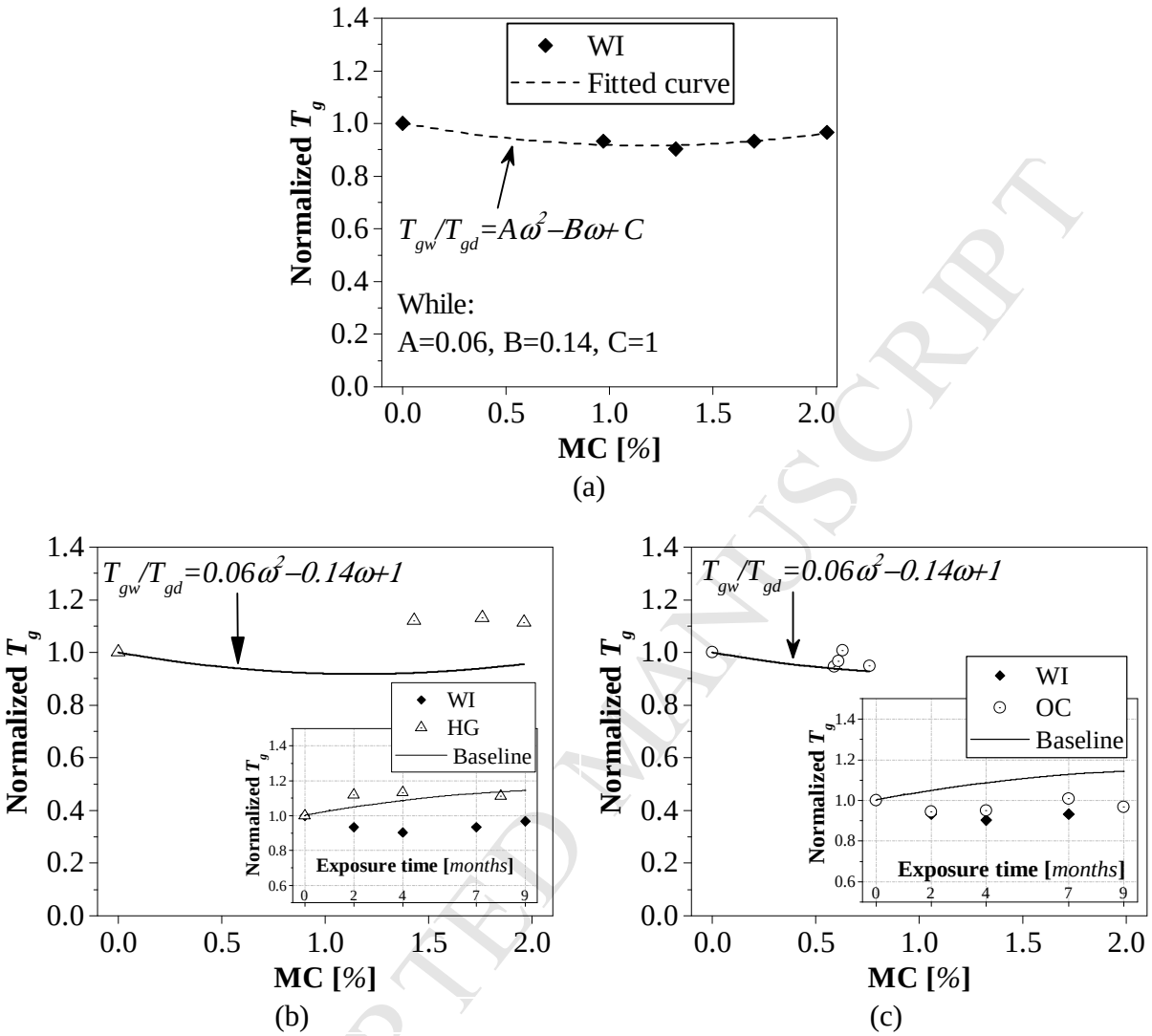

Fig 14. Changes of T_{g1} with moisture absorption in (a) WI; (b) HG; (c) OC specimens.